




## RESEARCH ARTICLE

Human-like enamel growth in *Homo naledi*

Patrick Mahoney<sup>1</sup>  | Gina McFarlane<sup>1</sup>  | Alberto J. Taurozzi<sup>2</sup> |  
 Palesa P. Madupe<sup>2,3</sup> | Mackie C. O'Hara<sup>1</sup> | Keneiloe Molopyane<sup>4,5</sup> |  
 Enrico Cappellini<sup>2</sup> | John Hawks<sup>4,6</sup>  | Matthew M. Skinner<sup>1</sup> | Lee Berger<sup>4,5,7</sup>

<sup>1</sup>Skeletal Biology Research Centre, School of Anthropology and Conservation, University of Kent, Canterbury, UK

<sup>2</sup>Section for GeoGenetics, Globe Institute, University of Copenhagen, Copenhagen, Denmark

<sup>3</sup>Human Evolution Research Institute, University of Cape Town, Rondebosch, South Africa

<sup>4</sup>Centre for the Exploration of the Deep Human Journey, University of the Witwatersrand, Johannesburg, South Africa

<sup>5</sup>The National Geographic Society, Washington, District of Columbia, USA

<sup>6</sup>Department of Anthropology, University of Wisconsin–Madison, USA

<sup>7</sup>The Carnegie Institution for Science, Washington, District of Columbia, USA

## Correspondence

Patrick Mahoney, Skeletal Biology Research Centre, School of Anthropology and Conservation, University of Kent, Canterbury, UK.

Email: [p.mahoney@kent.ac.uk](mailto:p.mahoney@kent.ac.uk)

## Funding information

Lyda Hill Foundation; National Geographic Society; The Royal Society and The Leverhulme Trust, Grant/Award Numbers: RPG-2018-226, RG110435; European Union's Horizon 2020, Grant/Award Numbers: 101026776, 101021361, 819960; European Commission, Grant/Award Number: 861389

## Abstract

**Objectives:** A modern pattern (rate and duration) of dental development occurs relatively recently during human evolution. Given the temporal overlap of *Homo naledi* with the first appearance of fossil *Homo sapiens* in Africa, this small-bodied and small-brained hominin presents an opportunity to elucidate the evolution of enamel growth in the hominin clade. Here we conduct the first histological study of two permanent mandibular canines and one permanent maxillary first molar, representing three individuals attributed to *H. naledi*. We reconstruct the rate and duration of enamel growth and compare these findings to those reported for other fossil hominins and recent humans.

**Materials and Methods:** Thin sections of each tooth were produced using standard histological methods. Daily and longer period incremental markings were measured to reconstruct enamel secretion and extension rates, Retzius periodicity, canine crown and molar cusp formation time.

**Results:** Daily enamel secretion rates overlapped with those from recent hominins. Canine crown formation time is similar to that observed in recent Europeans but is longer than canine formation times reported for most other hominins including *Australopithecus* and *H. neanderthalensis*. The extended period of canine formation appears to be due to a relatively tall enamel crown and a sustained slow rate of enamel extension in the cervical portion of the crown. A Retzius periodicity of 11 days for the canines, and nine days for the molar, in *H. naledi* parallel results found in recent humans. An 11-day periodicity has not been reported for Late Pleistocene *Homo* (*H. erectus*, *H. neanderthalensis*) and is rarely found in *Australopithecus* and *Paranthropus* species.

**Discussion:** Enamel growth of *H. naledi* is most similar to recent humans though comparative data are limited for most fossil hominin species. The high Retzius periodicity values do not follow expectations for a small-brained hominin.

## 1 | INTRODUCTION

Tooth enamel retains a growth record that can be accessed through histology and utilized to reconstruct enamel growth of hominin

permanent teeth (Bromage & Dean, 1985; Dean et al., 2001; Lacruz et al., 2008; Lacruz & Bromage, 2006; Reid & Dean, 2006; Smith et al., 2007; Smith et al., 2015; Xing et al., 2019). These studies indicate that enamel of permanent teeth typically formed rapidly and over

This is an open access article under the terms of the [Creative Commons Attribution](https://creativecommons.org/licenses/by/4.0/) License, which permits use, distribution and reproduction in any medium, provided the original work is properly cited.

© 2024 The Authors. *American Journal of Biological Anthropology* published by Wiley Periodicals LLC.

a shorter duration in *Australopithecus* and *Paranthropus* compared to recent humans. While enamel growth rates in Neandertals are debated (Guatelli-Steinberg et al., 2005; Ramirez Rozzi & Bermudez de Castro, 2004; Rosas et al., 2017; Smith et al., 2010), recent research indicates Neandertal milk teeth formed rapidly over a short period time and commenced emergence towards the advanced end of the eruption schedule displayed by recent humans (Mahoney et al., 2021). The slow pace of enamel growth among living humans is thought to have emerged relatively recently as it is not observed in *Homo erectus* (Dean et al., 2001).

*Homo naledi* is known from several localities within the Rising Star cave system of South Africa (Berger et al., 2015; Elliott et al., 2021; Hawks et al., 2017). Fossil remains from the Dinaledi Chamber are associated with a geochronological range between c335,000 and 241,000 years ago (Dirks et al., 2017; Robbins et al., 2021), while no direct estimate of age is available for other localities. The species is morphologically distinct from other hominin species or populations that existed in the late Middle Pleistocene, including Neandertals, Denisovans, early *H. sapiens* and some *H. erectus* (Berger et al., 2015; Dirks et al., 2017; Harvati & Reyes-Centeno, 2022; Hublin et al., 2017; Schroeder et al., 2017). The endocranial volumes of *H. naledi* crania range between 460 and 610 mL (Hawks et al., 2017; Holloway et al., 2018) and body mass estimates for adults average between 37 and 44 kg (Garvin et al., 2017). This combination indicates a relationship of brain to body size that is broadly similar to *Australopithecus* and *Paranthropus*, with an absolutely and relatively smaller brain size than *H. erectus*.

Brain size correlates tightly with dental development across primates (Smith, 1989). It is not surprising therefore that the slow pace of enamel formation in recent humans is not present in the smaller-brained australopiths (Dean et al., 2001; Lacruz & Bromage, 2006). Others have identified a strong relationship between the timing of enamel layers (Retzius periodicity) and encephalization when compared across fossil hominins (Hogg et al., 2020). Based upon these studies, the dental development of *H. naledi* should be similar to earlier hominins. Interestingly, observations from perikymata spacing indicate the lateral enamel of *H. naledi* anterior teeth formed in a way that was more similar to recent humans (Guatelli-Steinberg et al., 2018). However, lack of information about the number of days to form a perikyma has prevented the precise assessment of enamel growth rates and formation times. The sequence of permanent tooth emergence for a mandible of *H. naledi* included both modern and ancestral traits (Cofran & Walker, 2017). The emergence sequence of premolars followed by a second molar of *H. naledi* U.W. 101-377 is usually seen in recent humans, but the relatively late emergence of a canine is typical of Plio-Pleistocene hominins and chimpanzees (Cofran & Walker, 2017).

As part of a larger research program aimed at addressing several aspects of the evolutionary biology of *H. naledi*, we selected three isolated permanent teeth for invasive sampling. These teeth are a mandibular permanent canine (LC), another LC with incomplete cervical enamel, and an upper permanent first maxillary molar (UM1). These teeth come from three distinct chambers in the cave system and

represent three different depositional contexts, and therefore three different individuals. All present diagnostic morphology of *H. naledi*. Using histological methods, we reconstruct both the rate at which the enamel crown increased in thickness and height, and the duration over which a canine crown and molar cusps formed. Retzius periodicity (RP) values are calculated for each tooth.

## 1.1 | *Homo naledi*

The skeleton of *H. naledi* is a mosaic morphology of ancestral, derived, and unique traits (Berger et al., 2015; Garvin et al., 2017; Holloway et al., 2018). Its small brain is similar to *Australopithecus* (Garvin et al., 2017; Laird et al., 2017), but parts of the endocranium are organized in a way that is comparable to other species of *Homo* (Holloway et al., 2018). Hand and lower limb bones have traits that are shared with *Australopithecus* and *Homo* (Harcourt-Smith et al., 2015; Kivell et al., 2015; Marchi et al., 2017) and other parts of the skeleton show similar levels of mosaicism (Feuerriegel et al., 2017; Williams et al., 2017; VanSickle et al., 2018; see Bolter et al., 2020 for maturation of skeletal elements).

The *H. naledi* dental assemblage represents at least 15 individuals (Berger et al., 2015; Bolter et al., 2020; Bolter & Cameron, 2020). Molars display a simple crown morphology that increases in size posteriorly (M1 < M2 < M3) like *Australopithecus* and some early *Homo* (Berger et al., 2015). Premolars have a more complex morphology with tall crowns and well developed metaconids (Davies et al., 2020). Permanent teeth are similar to other *Homo* samples in their near absence of accessory traits but retain other traits that characterize Pliocene hominins (Irish et al., 2018). Deciduous teeth have a combination of morphological traits that in some cases resemble earlier hominins such as *Australopithecus*, *Paranthropus* and early *Homo*, but in others are unique to this taxon (Bailey et al., 2019).

Mandibular molar enamel is relatively thick like that of *P. robustus* and *A. africanus* (O'Hara, 2021; O'Hara et al., 2019; Skinner et al., 2016). The thick dental enamel does not follow the general trend towards a reduction in enamel thickness that characterizes the genus *Homo* over the past 2.5 million years (Lockey et al., 2020; Skinner et al., 2015). Chipping rates (Towle et al., 2017) and molar microwear (Ungar & Berger, 2018) indicate *H. naledi* could have consumed hard foods that may have included grit. Dental topography (Berthaume et al., 2018), large molar root surface areas (Kupczik & Skinner, 2018) and thick mandibular molar enamel (Skinner et al., 2016) suggest that *H. naledi* teeth resisted high loading stresses and/or crack propagation.

## 1.2 | Enamel secretion rates

Developing tooth crowns increase in thickness as enamel cells, called ameloblasts, deposit new matrix. Enamel matrix secretion is altered every 24-h in primates leading to alternating dark and bright lines (Boyd, 1989) or constrictions along the length of prisms (Li &

Risnes, 2004) named cross striations. Cross striations become visible when a tooth is prepared as a thin section and viewed under a microscope. The distance between adjacent pairs of cross striations along an enamel prism is the amount of enamel deposited by ameloblasts over one 24-h period (e.g., Schour & Poncher, 1937; Zheng et al., 2013). This can be expressed as a daily secretion rate (DSR) that is measured in microns per day (e.g., Reid et al., 1998). An enamel DSR is therefore a measure of the rate that enamel increases in thickness in a particular area of the developing crown. Comparisons between individuals are usually restricted to similar enamel regions and the same tooth types (e.g., Beynon et al., 1991; Dean, 1998).

Recent humans and extant great ape teeth typically display a trajectory of enamel growth (e.g., Beynon et al., 1991; Mahoney, 2008), whereby DSRs commence relatively slowly near the enamel-dentin junction (EDJ) and accelerate towards the future outer enamel surface. This trajectory has been observed in *Australopithecus*, *Paranthropus*, *H. habilis*, *H. erectus* and the Middle Pleistocene Xujia Yao juvenile (Lacruz & Bromage, 2006; Lacruz et al., 2008; Xing et al., 2019 their supplementary table 3). The underlying rate at which ameloblasts deposit enamel is much faster in some early hominin species when compared to recent humans, especially towards the outer cuspal enamel surface of molars in *Paranthropus* (*P. aethiopicus*, *P. boisei*, *P. robustus*) and *A. africanus* (Lacruz, 2007; Lacruz et al., 2008; Lacruz & Bromage, 2006). High DSRs in these hominin fossils have been linked to greater tooth size and enamel thickness (Lacruz et al., 2008).

### 1.3 | Enamel extension rates

Extension rates are a proxy for the rate at which a developing crown gains height as new ameloblasts are activated along the EDJ (Dean, 1998; Shellis, 1984). In recent humans, faster extension rates occur nearer the dentin horn and slower rates are usually present nearer the tooth cervix (Guatelli-Steinberg et al., 2012; Mahoney, 2015). Extension rates are expressed in microns per day.

Several factors are known to influence extension rates within recent humans. Initial rates relate to the length of the EDJ (Shellis, 1984). Taller permanent incisors extend faster than shorter molars, and enamel on molars with longer EDJs will initially spread quickly over the cuspal region compared to shorter molars (Guatelli-Steinberg et al., 2012). Canines of recent humans with slower growth in cervical enamel have lower RP values, while those with higher RPs do not show the same abrupt slowing in pace in cervical regions (McFarlane et al., 2014; Reid & Ferrell, 2006).

Only a few studies have reported enamel extension rates for hominin fossils. Rates for the enamel crown of a lower canine of *Paranthropus robustus* (SK 63), and a first molar crown of *H. erectus* lie within the range of recent humans (Dean, 2009). An average crown extension rate for one canine and two upper molars of Neandertal lay just above the upper most range of extension rates from a sample of Europeans and South Africans (Smith et al., 2010).

### 1.4 | Crown formation times

Because enamel forms incrementally and retains a record of that growth it is possible to reconstruct the total time taken by ameloblasts to form a tooth crown or cusp (e.g., Dean & Beynon, 1991). When compared to a known age-at-death, histological reconstructions of crown formation time (CFT) are accurate to within a few days or weeks for humans (Antoine et al., 2009).

Dean et al. (2001) reconstructed CFT from regression equations, perikymata and estimated Retzius periodicities, and reported shorter crown formation times for permanent incisors and canines from *H. erectus*, *Australopithecus* and *Paranthropus* compared to recent humans. Comparatively short CFTs have been reported for the post-canine teeth of *Australopithecus* (Smith et al., 2015). The total period over which Neandertal canines formed was shorter than that of recent humans (Smith et al., 2010) while the lateral enamel of their anterior teeth formed over a period that is like that of modern humans (Guatelli-Steinberg et al., 2005). The Middle Pleistocene Xujia Yao juvenile has an upper canine formation time (Xing et al., 2019) that lies within the range of recent humans (Reid & Dean, 2006), while the CFT of the Irhoud 3 juvenile lies above the range of modern Europeans (Smith et al., 2007).

### 1.5 | Retzius periodicity

Retzius lines are a long-period incremental marking formed by ameloblasts (Retzius, 1837). The number of days of enamel secretion between two adjacent lines is termed Retzius periodicity (RP) (see Section 2.4 for calculating RP). Among hominins, RP of permanent teeth varies between individuals, from 5 to 12 or 13 days (McFarlane et al., 2021; Reid & Dean, 2006; Smith et al., 2015). McFarlane et al.'s (2021) study of  $n = 223$  recent human teeth revealed RP can vary along the tooth row within an individual, with molars having a lower median RP of 8 days compared to the median RP of 10 days for anterior teeth. Their finding is consistent with that of Reid and Dean (2006) who reported a higher mean value in anterior teeth compared to the mean RP of molars within a population. Together, these results indicate that it is important during comparisons of RP that include recent humans, to restrict those comparisons to the same tooth classes. Whether there is similar variation in RP along the tooth row in other hominin species, or the great apes, has not yet been determined.

The mean RP of recent humans is higher than that of other hominins (Hogg et al., 2020) though RP values of individual teeth for some species (e.g., *A. anamensis*, *P. robustus*, *A. africanus*; Smith et al., 2015) and the Middle Pleistocene Xujia Yao juvenile (Xing et al., 2019) lie within the upper range of values reported for recent humans. Although the underlying cause of the lines is unknown, inter-specific analyses of mean or modal RPs reveal a positive correlation between RP and mean body mass of hominoids (Smith, 2008), Plio-Pleistocene hominins (Lacruz et al., 2008), and anthropoid primates (Bromage et al., 2009). Hominins as a group follow the RP-body mass correlation when examined alongside hominoids, but the inter-specific correlation with mass is not significant within hominins (Hogg

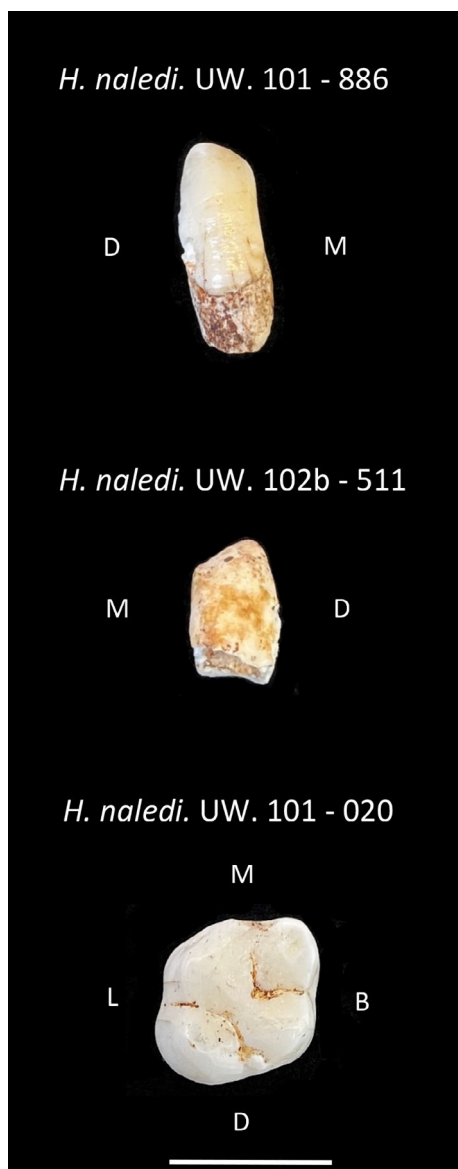


**FIGURE 1** Photographs of the selected *Homo naledi* teeth. Top row: *H. naledi*. UW. 101-886 lower right permanent canine, labial view. Middle row: *H. naledi*. UW. 102b-511 lower left permanent canine, labial view. Lower row: *H. naledi*. UW. 101-020 upper left permanent first molar, occlusal view. M, mesial; D, distal; L, lingual; B, buccal. Scale bar is 1 cm.

et al., 2020). There is a significant and positive relationship between hominin RP and an index of cranial capacity indicating a potential relationship with encephalization whereby larger-brained species have a higher RP (Hogg et al., 2020).

## 2 | SAMPLES AND METHODS

### 2.1 | Samples

Three isolated permanent teeth assigned to *H. naledi* were selected for analysis (Figure 1). U.W. 101-886 is a mandibular right canine from the Dinaledi Chamber excavated from a context that includes the

commingled remains of at least five *H. naledi* individuals. This tooth has a probable antimere (U.W. 101-1126) within the Dinaledi collection (Deleuzene et al., 2023). The second tooth selected for analysis was U.W. 102b-511, a mandibular left canine from the Lesedi Chamber with incomplete cervical enamel (Hawks et al., 2017). The U.W. 102b-511 canine appears to be still forming at the time of death. This tooth is associated with two permanent incisors, one premolar crown and one deciduous molar, all representing a subadult individual from the 102b locality. The third tooth selected for analysis was U.W. 101-020, a maxillary left first molar recovered from the surface of the Hill Antechamber (Elliott et al., 2021). Multiple criteria were used in the selection of these three teeth for analysis. Each represents a different individual of *H. naledi* separated from distinct chambers of the Rising Star cave system. Occlusal wear is minimal or absent on each of the teeth, maximizing the extent of evidence from histological sectioning. First molar and canine teeth were selected to sample the lifespan from first molar enamel initiation to canine crown completion.

These teeth are from three distinct depositional situations. Geochronological work in the Dinaledi Chamber suggests that the fossil material from this situation is between 335,000 and 241,000 years old (Dirks et al., 2017; Robbins et al., 2021). It is not clear whether this age range also encompasses the skeletal material from the Hill Antechamber (Elliott et al., 2021), and no estimate of geological age has been presented for material from the Lesedi Chamber (Hawks et al., 2017). Each of these teeth has morphology diagnostic of *H. naledi*, as does surrounding skeletal material, but it is not yet clear whether these represent the same population or may represent populations that lived at different times.

### 2.2 | Comparative data

Extension rates were calculated for a sample of recent humans from the UCL-Kent collection and the Newcastle collection. The UCL-Kent collection was obtained from dental surgeries in northern Britain in the 1960's and 1970's. The sex of some individuals was known but otherwise all individuals were anonymous. Thin sections were produced for this sample in the Histology Laboratory, University of Kent. Ethical approval for histology research on this collection of teeth was obtained from the UK National Health Service research ethics committee (REC reference: 16/SC/0166; project ID: 203541). The Newcastle collection was collected by Dr Cynthia Reid at Witwatersrand Dental Hospital in South Africa between 1986 and 1987. The Newcastle collection consists of existing thin sections. Both collections are curated in the Histology Laboratory, University of Kent.

Comparative DSRs, CFT and RP for recent humans and a range of fossil hominins were taken from the published literature. Additionally, mean canine DSRs were calculated for recent humans and *P. robustus* using regression equations provided by Chris Dean (pers' comm).

### 2.3 | Lab protocol and environment

The teeth were sectioned (see Section 2.4) in the laboratory dedicated to the extraction and the recovery of ancient proteins at the Globe

Institute, University of Copenhagen, Denmark. Thin sections from these teeth were transported to the histology laboratory at the University of Kent, UK. The laboratory design and the procedures adopted in the lab at the University of Copenhagen are conceived to minimize the contamination of ancient biomolecules with modern exogenous contaminants. The laboratory is under positive air pressure, and nightly UV-irradiated. All operators working in the laboratory are required to wear extensive personal protective equipment which include a full body suit, additional sleeves, hairnet, face mask, shoe covers and two pairs of gloves. Sample preparation was performed within a class II biosafety cabinet.

## 2.4 | Histology

Thin sections from these teeth were transported to the histology laboratory at the University of Kent. Teeth were sectioned through the midline of the canines and the distal cusps of the molar passing through the dentin horn. Standard procedures (see Mahoney et al., 2022) were employed but with one modification to accommodate subsequent chemical and molecular analyses. Specifically, teeth were embedded in crystal bond (Agar Scientific) before additional embedding in resin (Buehler EpoxiCure), so that the sectioned portions of each tooth could be removed from the resin.

Teeth were cut with a diamond wafering blade using a Buehler IsoMet low speed machine. Sections were fixed to a microscope slide (Evo Stick resin), ground with pads of decreasing grit sizes (P400, P600, P1200), polished with an aluminium oxide powder (Buehler Micro-Polish), cleaned in an ultrasonic bath, dehydrated in 95% ethanol, cleared (Histoclear) and mounted with a cover slip (DPX). Each section was examined with a high-resolution microscope (Olympus® BX53) and microscope camera (Olympus® DP25). Images were obtained and analyzed in CELL® Live Biology imaging software. Standard histology variables were calculated.

Daily enamel secretion rates in microns per day were calculated for inner, mid, and outer cuspal and lateral regions of each tooth. Rates were measured along the long-axis of prisms. Five consecutive days of enamel secretion, measured in multiple locations within each region, was used to calculate an overall mean value for that region.

Enamel extension rates in  $\mu\text{m}$  per day were calculated for the length of the EDJ of the canines, and molar. The method is based on root extension reported by Dean and Vesey (2008) with rates calculated at fixed intervals of 200, 500, and 1000  $\mu\text{m}$  from the dentin horn, and every 500  $\mu\text{m}$  thereafter, continuing to the enamel cervix. Figure 2 shows the way these rates were recorded for U.W. 101-886 LC (magnification of 20 $\times$ ). Point A is located upon the EDJ. The white dashed line traces an enamel prism path towards the outer enamel surface for a distance of 200 microns away from the EDJ to point B. The dark line commencing at B traces the shape of an accentuated marking back to the EDJ indicated by point C. The distance in microns between A and C along the EDJ, divided by the time taken to form the 200-micron prism length, gives the extension rate in microns per day.

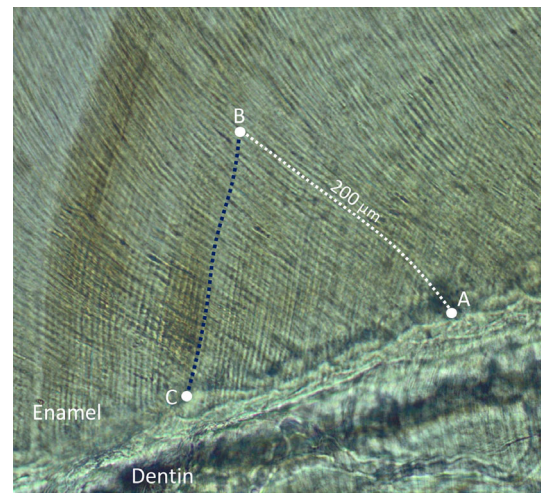


**FIGURE 2** Calculating enamel extension rates for U.W. 101-886 mandibular canine. See methods for details.

Crown formation time for the U.W. 101-886 canine was calculated using standard methods (e.g., Mahoney et al., 2007). Formation time for maxillary molar distal cusps is less frequently reported in the literature (e.g., Smith et al., 2015) and the distal-lingual cuspal enamel of U.W. 101-020 was slightly worn. For this distal cusp we reconstructed cuspal enamel (O'Hara & Guatelli-Steinberg, 2022). This method is appropriate for reconstructing wear facets on posterior teeth when the enamel is minimally worn, and the borders of the wear facet can be easily identified in order to extrapolate the unworn condition. We report cuspal formation time for both the distal-lingual and distal-buccal cusp so that these data can be accessed by other researchers.

Canine and molar cuspal enamel formation time was calculated using the formula: enamel thickness  $\times$  correction factor / mean daily rate of secretion. The correction factor accounts for changes in prism length resulting from prism decussation (Risnes, 1986). A correction factor of 1.05 was used (e.g., Mahoney, 2008; Risnes, 1986; Schwartz et al., 2003). Cuspal enamel thickness was measured from the tip of the dentin horn to the outermost tip of the enamel. For the molar distal-lingual cusp we used the mid-enamel region DSR from the distal-buccal cusp. Lateral and cervical enamel formation time was calculated by multiplying the number of Retzius lines by the periodicity. Where adjacent Retzius lines were indistinct, enamel prism lengths were divided by secretion rates in that region. The total enamel formation time was calculated by the sum of the time taken to form the cuspal, lateral and cervical enamel.

Retzius periodicity was calculated in two standard ways in lateral enamel (Mahoney et al., 2020). For the U.W. 102b-511 lower canine, we counted daily cross-striations along a prism between two adjacent Retzius lines (Section 3.4 for images). For the other canine and the molar, RP was calculated from prism lengths divided by local DSRs (e.g., Dean et al., 1993; Mahoney et al., 2007; Schwartz et al., 2001; Smith, 2008). The distance between four to six adjacent Retzius lines was measured, corresponding to three to five repeat intervals

respectively, and divided by three or five. This distance between two adjacent Retzius lines was then divided by the grand mean DSR to yield an RP value.

## 2.5 | Analyses

Data are described through mean values, standard deviations, and ranges. A linear regression analysis is conducted on log-transformed mean RP and mean encephalization of hominins.

## 3 | RESULTS

### 3.1 | Enamel secretion rates

Mean DSRs for the U.W. 101-886 and U.W. 102b-511 canines, and the U.W. 101-020 molar, increased towards the outer enamel surface relative to the inner and mid-enamel regions (Tables 1 and 2). Mean secretion rates for cuspal and lateral regions of the canines and molar are slightly higher than mean rates reported from equivalent regions in recent humans though DSRs from the *H. naledi* dental samples lie well within the range of recent humans (Tables 1 and 2).

Mean rates for the molar of *H. naledi* are slightly higher than the mean DSRs reported for molars from *H. erectus*. However, the range of DSRs from *H. naledi* overlap with *H. erectus* in outer cuspal enamel, and the Atapuerca hominins in lateral enamel regions (Table 2). The high DSRs that are present in the outer cuspal enamel of molars from some australopiths (*P. robustus*, *P. aeithiopicus*, *P. boisei*, and *A. africanus*) and the canine of SK 63 (*P. robustus*) are not present in *H. naledi* (Figure 3, Table 2).

### 3.2 | Enamel extension rates

Mean extension rates for the U.W. 101-886 and U.W. 102b-511 canines lie within the range of rates from our sample of recent humans (Figure 4a; see Table S3 for data). U.W. 101-886 extended in height for a longer period compared to the recent human canines, which occurred because the enamel crown was relatively tall with a long EDJ (Table S4 for data). Rates for the final 3 mm (from 10.5 to 13.5 mm) of cervical crown extension for U.W. 101-886 lay between 2.9 and 3.5  $\mu\text{m}/\text{day}$ . These rates were slow compared to the mean rates of 3.5–4.1  $\mu\text{m}/\text{day}$  present in the final 3 mm (from 7.5 to 10.5 mm) of crown extension in our comparative sample of recent humans. The most cervical enamel was missing from U.W. 102b-511 so final extension rates were not calculated for this portion of this LC.

The U.W. 101-020 molar extended in height at a rate that lies within the range of rates from a sample of recent human maxillary first molars (Figure 4b; Table S5 for data). Rates for the final 2 mm (from 4.5 to 6.5 mm) of cervical crown extension for U.W. 101-020 lay between 3.0 and 5.1  $\mu\text{m}/\text{day}$ . These cervical extension rates were slow compared to the mean crown extension rates of 4.8–5.6  $\mu\text{m}/\text{day}$  from an equivalent region of enamel in our comparative sample of recent humans.

### 3.3 | Formation times

The U.W. 101-886 canine formed over 2014 days (5.76 years; Table S6). This CFT lies above the range of LC formation times reported for recent South African humans, australopiths and Neanderthals but lies within the range of times reported for recent Europeans (Table 3).

**TABLE 1** Canine enamel daily enamel secretion rates in microns per day for U.W. 101-886 and U.W. 102b-511 (bold) and a comparative sample of recent humans (see Table S1 for inner enamel).

Enamel region	Species	Sex	n	Mean	SD	Min	Max	Source
Middle cuspal	<b><i>H. naledi</i></b>		2	<b>4.26</b>	<b>0.46</b>	<b>3.84</b>	<b>4.83</b>	This study
	Recent humans	M	33	3.72	0.38	2.91	4.58	Aris et al., 2020
		F	33	3.81	0.31	2.86	4.29	Aris et al., 2020
Outer cuspal	<b><i>H. naledi</i></b>		2	<b>5.16</b>	<b>0.55</b>	<b>4.01</b>	<b>5.56</b>	This study
	Recent humans		19	4.92	0.42	4.18	5.77	Schwartz et al., 2001
	Recent humans	M	27	4.17	0.5	3.42	5.05	Aris et al., 2020
		F	31	4.31	0.48	3.16	5.37	Aris et al., 2020
Middle lateral	<b><i>H. naledi</i></b>		2	<b>4.11</b>	<b>0.31</b>	<b>3.69</b>	<b>4.59</b>	This study
	Recent humans	M	44	3.65	0.33	2.99	4.42	Aris et al., 2020
		F	41	3.8	0.31	2.86	4.29	Aris et al., 2020
Outer lateral	<b><i>H. naledi</i></b>		2	<b>4.37</b>	<b>0.35</b>	<b>4.01</b>	<b>4.85</b>	This study
	Recent humans		19	4.38	0.32	3.98	4.97	Schwartz et al., 2001
	Recent humans	M	42	4.05	0.37	3.35	4.75	Aris et al., 2020
		F	40	4.15	0.4	3.03	4.81	Aris et al., 2020

Note: *H. naledi* buccal and lingual enamel rates are combined.

**TABLE 2** Molar enamel daily enamel secretion rates for U.W. 101-020 (**bold**) and the comparative sample of recent and fossil hominins (cervical enamel DSRs are in Table S2).

Enamel region	Species	Tooth	n	Mean	SD	Source
Middle cuspal	<b><i>H. naledi</i><sup>a</sup></b>	<b>UM1</b>	<b>1</b>	<b>4.83</b>	<b>0.33</b>	<b>This study</b>
	Recent humans	LMs	10	4.50	0.55	Lacruz & Bromage, 2006
	Recent humans	U/LMs	15	4.30	0.70	Beynon et al., 1991
	Recent humans	LM1	15	4.15	0.56	Mahoney, 2008
	<i>H. erectus</i>	LMs	2	4.46		Lacruz et al., 2008
	<i>P. robustus</i>	LMs	4	6.12	0.56	Lacruz & Bromage, 2006
	<i>A. africanus</i>	LMs	4	5.80	0.30	Lacruz & Bromage, 2006
	<i>A. anamensis</i>	U/LMs	2	5.04		Lacruz et al., 2008
	<i>A. afarensis</i>	LMs	3	4.66		Lacruz et al., 2008
	<i>P. aethiopicus</i>	LM3	1	5.31		Lacruz et al., 2008
<i>P. boisei</i>	LMs	4	5.74		Lacruz et al., 2008	
Outer cuspal	<b><i>H. naledi</i><sup>a</sup></b>	<b>UM1</b>	<b>1</b>	<b>5.31</b>	<b>0.31</b>	<b>This study</b>
	Recent humans	U/LMs	12	5.10	0.70	Beynon et al., 1991
	Recent humans	LM1	15	4.55	0.61	Mahoney, 2008
	Recent humans	M	10	5.25	0.58	Lacruz & Bromage, 2006
	<i>H. erectus</i>	LMs	2	5.19		Lacruz et al., 2008
	<i>P. robustus</i>	LMs	5	7.25	0.44	Lacruz & Bromage, 2006
	<i>A. africanus</i>	LMs	5	6.62	0.55	Lacruz & Bromage, 2006
	<i>A. anamensis</i>	U/LMs	2	5.47		Lacruz et al., 2008
	<i>A. afarensis</i>	LMs	3	5.84		Lacruz et al., 2008
	<i>P. aethiopicus</i>	LM3	1	6.53		Lacruz et al., 2008
<i>P. boisei</i>	LMs	4	7.15		Lacruz et al., 2008	
Middle lateral	<b><i>H. naledi</i><sup>a</sup></b>	<b>UM1</b>	<b>1</b>	<b>4.55</b>	<b>0.31</b>	<b>This study</b>
	Recent humans	M	10	4.30	0.50	Lacruz & Bromage, 2006
	Recent humans	U/LMs	15	4.00	0.40	Beynon et al., 1991
	<i>H. erectus</i>	LMs	2	4.20		Lacruz et al., 2008
	Atapuerca hominins <sup>b</sup>	M3	1	4.37	0.41	Modesto-Mata et al., 2020
	<i>P. robustus</i>	LMs	5	5.63	0.27	Lacruz & Bromage, 2006
	<i>A. africanus</i>	LMs	5	5.25	0.39	Lacruz & Bromage, 2006
	<i>A. afarensis</i>	LMs	3	4.76		Lacruz et al., 2008
	<i>P. aethiopicus</i>	LM3	1	4.86		Lacruz et al., 2008
	<i>P. boisei</i>	LMs	2	4.99		Lacruz et al., 2008
Outer lateral	<b><i>H. naledi</i></b>	<b>UM1</b>	<b>1</b>	<b>5.26</b>	<b>0.28</b>	<b>This study</b>
	Recent humans	U/LMs	13	5.00	0.50	Beynon et al., 1991
	Recent humans	M	10	4.80	0.67	Lacruz & Bromage, 2006
	<i>H. erectus</i>	LMs	3	4.86		Lacruz et al., 2008
	Atapuerca hominins <sup>b</sup>	LM	4	4.77	0.29	Modesto-Mata et al., 2020
	<i>P. robustus</i>	LMs	5	6.59	0.27	Lacruz & Bromage, 2006
	<i>A. africanus</i>	LMs	6	6.11	0.37	Lacruz & Bromage, 2006
	<i>A. afarensis</i>	LMs	2	5.32		Lacruz et al., 2008
	<i>P. aethiopicus</i>	LM3	1	5.52		Lacruz et al., 2008
	<i>P. boisei</i>	LMs	5	5.84		Lacruz et al., 2008

<sup>a</sup>Data for distal cusps combined.<sup>b</sup>Data for outer lateral enamel is for an M1, M2 and M3 combined to produce mean and SD.

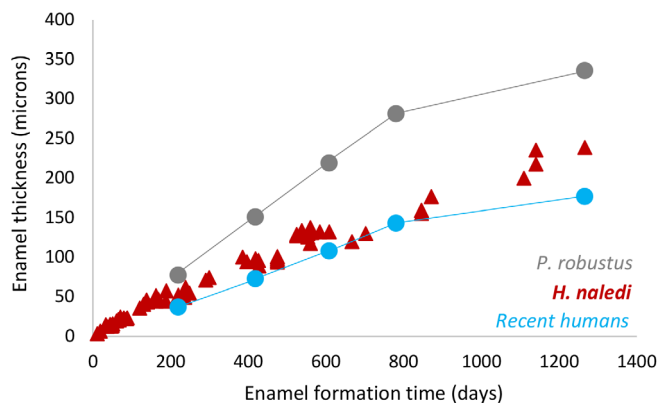


**FIGURE 3** Scatter plot illustrating the rate of canine enamel formation. The plot illustrates that *P. robustus* (SK 63) has a faster rate of enamel secretion compared to *H. naledi* (U.W. 101-886) and recent humans producing a greater depth of enamel thickness in a shorter period. The plot is created from multiple DSR measurements from the *H. naledi* canine, and mean DSRs for the same region in a sample of recent humans and *P. robustus* that were calculated from regression equations provided by Chris Dean (pers. Comm).

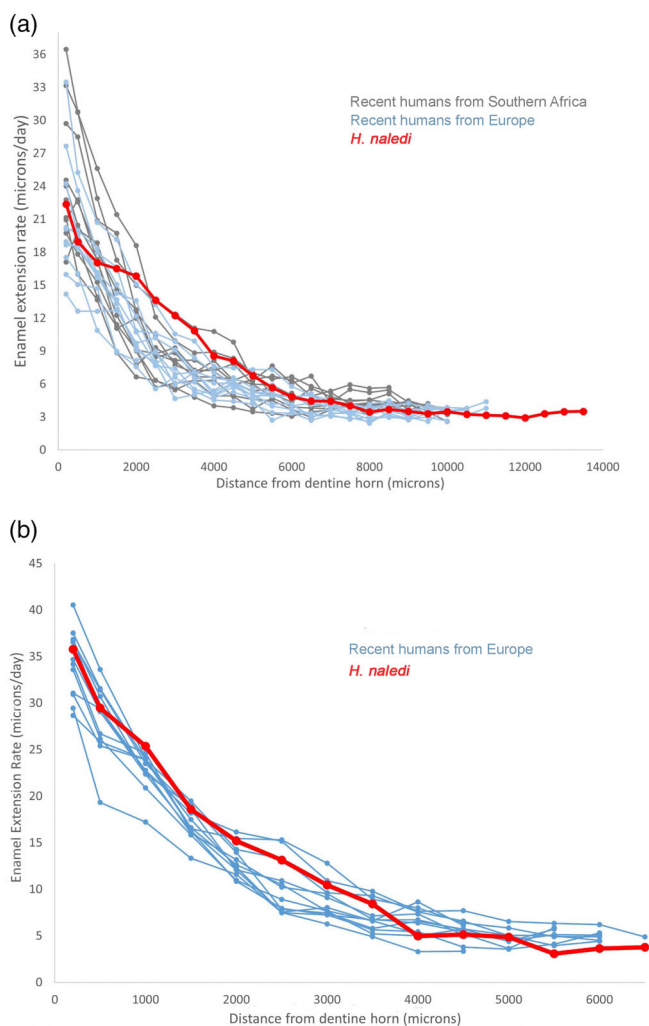


**FIGURE 4** Extension rates compared between *H. naledi* and recent humans for (a) canines, and (b) molars.

The reconstructed upper M1 (U.W. 101-020) distal-lingual cusp formed over 1187 days and the distal-buccal cusp formed over 597 days. The UM1 distal-lingual cusp formation time is higher than that reported for recent humans (mean = 1088 days), *A. africanus* (959 days) and *P. robustus* (758 days) (Smith et al., 2015).

### 3.4 | Retzius periodicity

The U.W. 102b-511 canine had an 11-day periodicity that was calculated from two direct counts of cross stations (Figure 5). Periodicity for the U.W. 101-886 canine was 11 days, and the U.W. 101-020 molar had a nine-day periodicity.

Periodicities of nine and 11 days for *H. naledi* lie within the range of RPs reported for recent humans (McFarlane et al., 2021), *A. anamensis* and *A. africanus* (Smith et al., 2015). The *H. naledi* RPs overlap with those from *P. robustus*, the one value reported for the Middle Pleistocene Xujiayao juvenile (Xing et al., 2019), and the uppermost value from fossil *H. sapiens*, Irhoud 3 (Smith et al., 2007) (Figure 6). When excluding any potential variation in RP due to tooth type, RPs of 11 days for the two *H. naledi* canines lie above the modal value of nine days reported for modern human canines (McFarlane et al., 2021; Reid & Dean, 2006). An RP of nine days for the *H. naledi* molar is higher than the modal value of eight days reported for human molars (McFarlane et al., 2021; Reid & Dean, 2006).

## 4 | DISCUSSION

### 4.1 | Enamel growth rates

The trajectory of ameloblast secretion for these *H. naledi* canines and molar is typical of permanent enamel growth in most hominoids. Enamel was secreted rapidly towards the outer enamel surface relative to regions nearer the EDJ which has been observed in Miocene hominoids and recent humans, as well as extant great apes (Beynon et al., 1991; Mahoney et al., 2007; Schwartz et al., 2001). Each crown gained height quickly near the dentin horn and slowly towards the cervix, which has been reported for a lower canine of *Paranthropus robustus* (SK63), first molars of Neandertal, *H. erectus* (Dean, 2009) and teeth of recent humans (Guatelli-Steinberg et al., 2012; Mahoney, 2015). Faster DSRs and extension rates in molars compared to canines of *H. naledi* are similar to the variation in enamel growth rates that we observed between these tooth types in recent humans (Figures S1, S2).

Enamel secretion rates of *H. naledi* resemble those of recent hominins. DSRs near the EDJ were, on average, only slightly faster in *H. naledi* than recent humans and *H. erectus*. Those from molar outer enamel regions were much lower than the DSRs reported for *Paranthropus* and *Australopithecus* (Lacruz et al., 2008; Lacruz & Bromage, 2006). It is important to note that these observations have been based on very few Pleistocene hominin teeth (which includes *H. habilis*, *H. erectus*, *H. antecessor*, *H. heidelbergensis*, *H. floresiensis*).

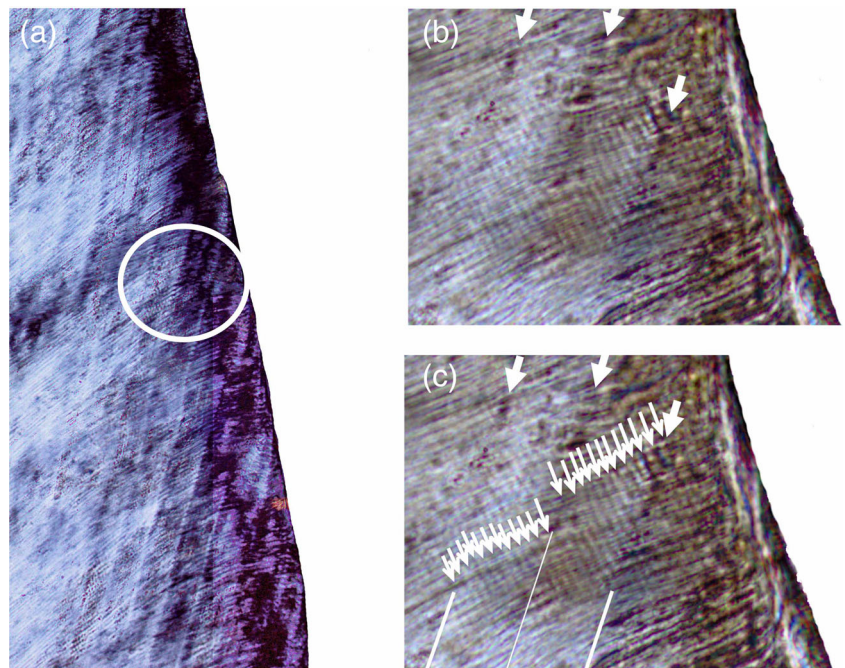


**TABLE 3** Histologically derived hominin mandibular canine formation times.

Species	Tooth	n	Days	Source
<i>H. naledi</i> U.W. 101-886	LC	1	2014	This study
Recent humans—Europe	LC	13	1993–2139 <sup>a</sup>	Reid & Dean, 2006
Recent humans—South Africa	LC	25	1638–1750 <sup>a</sup>	Reid & Dean, 2006
<i>H. sapiens</i> —fossil (Irhoud 3)	LC	1	2439	Smith et al., 2007
<i>Homo</i> sp.—Xujia Yao	UC	1	1812	Xing et al., 2019.
<i>H. erectus</i> —Sanigran	UC	1	1377–1653	Dean et al., 2001
Neandertal	LC	1	1305	Smith et al., 2010.
Neandertal	UC	1	1228–1241	Smith et al., 2010
<i>P. robustus</i> (SK 63)	LC	1	1273	Dean et al., 1993
<i>Australopithecus</i>	LC	5	1360–1646	Dean et al., 2001
<i>Paranthropus</i>	LC	6	1040–1246	Dean et al., 2001
<i>Early homo</i> (SK 27)	UC	1	1497–1803	Dean et al., 2001
<i>A. anamensis</i>	LC	1	988	Smith et al., 2015
<i>A. anamensis</i>	LC	1	1280–1499	Smith et al., 2015
<i>A. africanus</i>	UC	1	1014	Smith et al., 2015
<i>P. robustus</i>	LC	1	938	Smith et al., 2015
<i>P. robustus</i>	LC	1	1558	Smith et al., 2015
<i>P. robustus</i>	UC	1	818	Smith et al., 2015

<sup>a</sup>Range calculated from their reported mean and one SD.

**FIGURE 5** Retzius periodicity for the U.W. 102b-511 mandibular canine. (a) Retzius lines at a magnification of 4× in the U.W. 102b-511 canine. (b) Close up (20×) of A, showing three Retzius lines indicated by large white arrows with cross striations running between the three adjacent lines. (c) Image B duplicated with two direct counts of cross striations illustrated by small white arrows. Each count of cross striations between two adjacent Retzius lines gives an RP of 11 days (12 cross striations minus 1 = RP of 11 days). Zoom in to count cross striations.



For this reason, it remains to be seen whether the similarities in enamel growth rates with recent humans are a shared derived pattern or whether these similarities may instead be plesiomorphic.

The rate at which each of the *H. naledi* crowns gained height was within the range of our sample of European and South African humans except for cervical enamel. The U.W. 101-886 canine had a very slow rate of cervical extension. This is consistent with observations from the distribution of perikymata on the lateral surface of *H.*

*naledi* permanent anterior teeth, which suggested the pace of formation might be slower in cervical enamel compared to other hominins (Guatelli-Steinberg et al., 2018).

When variation in crown height is controlled, canines of recent humans that have slower growth rates in cervical enamel tend to have lower RPs, while those with higher RPs do not show the same abrupt slowing in the pace of enamel formation in this region (McFarlane et al., 2014; Reid & Ferrell, 2006). Modern human molars that have taller

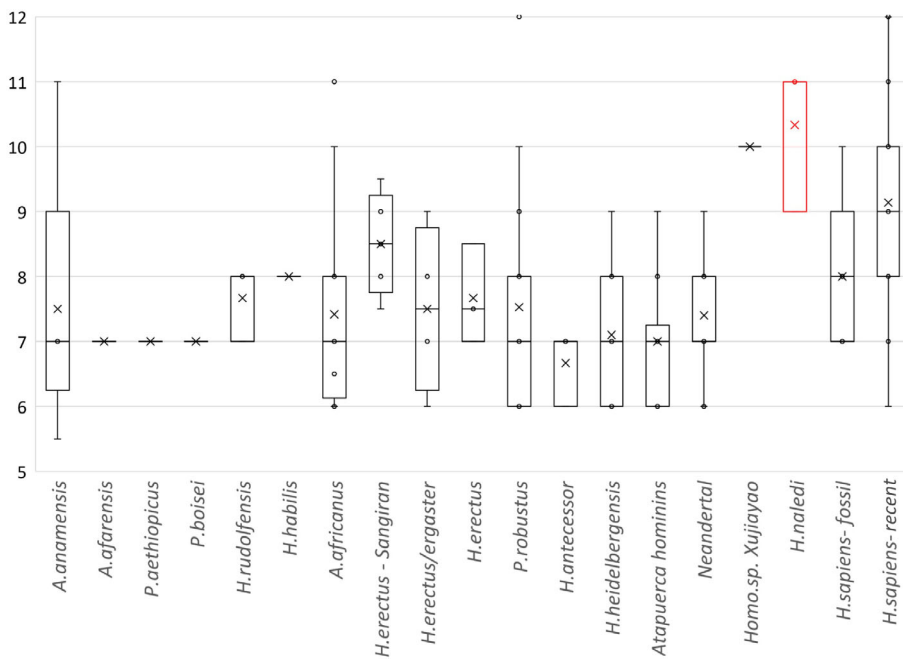


**FIGURE 6** Retzius periodicity in hominins (see Table S7 for data and sources).

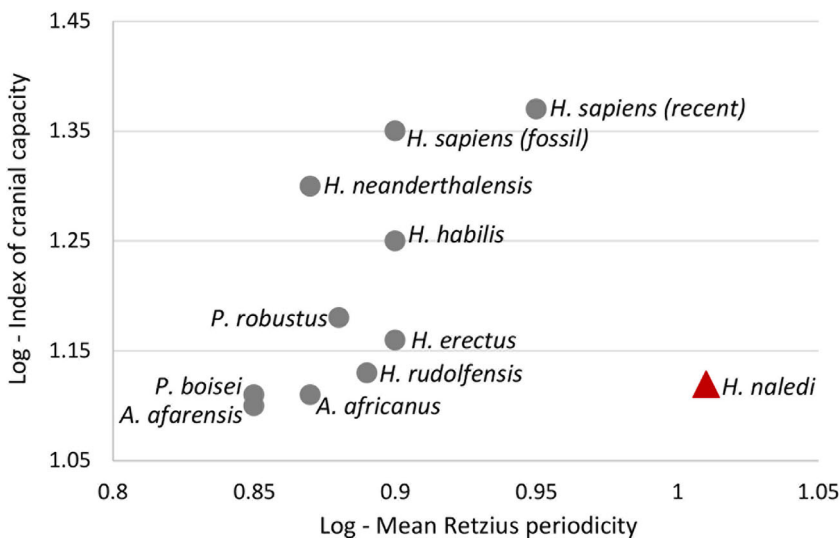


**FIGURE 7** Index of mean cranial capacity and mean Retzius periodicity for hominins. See Table S8 for data and sources.

crowns, and modern human anterior teeth with more tightly compacted perikymata in the cervical portion of the tooth, both tend to have faster initial extension rates at the dentin horn (Guatelli-Steinberg et al., 2012). It is difficult to know if the relationships observed in humans would hold for *H. naledi* as the longer period of cervical extension probably alters things. If the U.W. 101-886 canine followed the recent human pattern, then the slow pace of cervical growth would fit a lower RP not the higher RP we report. It is clear that the initial extension rate of these *H. naledi* canines is not fast compared to our human comparative sample.

## 4.2 | Crown formation time

The U.W. 101-886 lower canine formed over a longer period compared to CFTs reported for all hominins except those from recent

Europeans and the Irhoud 3 fossil human child. It is likely that the slow rate of cervical extension (Figure 4a) combined with a long EDJ (Table S4 for data) to produce a high CFT for *H. naledi*. The EDJ length of 12.86 mm for the U.W. 101-886 canine lay just above the EDJ lengths that ranged between 7.64 to 12.66 mm (mean = 10.34 mm) in a sample of recent human lower canines (Table S4).

## 4.3 | Retzius periodicity

An 11-day periodicity for the U.W. 101-886 and U.W. 102b-511 canines is not unusual. It lies within the upper range of RPs reported for recent humans (McFarlane et al., 2021) and it has been observed in *A. africanus* and *A. anamensis* (Smith et al., 2015). Furthermore, a 12-day periodicity is present in recent humans and was observed in

*P. robustus* (McFarlane et al., 2021; Smith et al., 2015). However, these high RP values are not representative of the RPs that are typical of fossil hominins. Analyses of currently available data indicate that when fossil hominins are considered as a group, they have a modal RP of 7 days (Table S7), and a mean periodicity that is significantly lower than the mean RP of recent humans (Hogg et al., 2020). Australopiths have a modal RP of 7 days (Table S7).

Accumulating evidence indicates that RP reflects an underlying biological cycle that acts upon the mammalian hypothalamus. It is hypothesized that the cycle regulates cell growth when compared between mammalian species (Bromage et al., 2009), and it has been observed that RP relates to body mass and maturation rate within human adolescents (Mahoney et al., 2022). These findings have been important for developing ideas about the evolution and pace of primate life history (Bromage et al., 2012), whereby the higher mean RP of recent humans relative to other hominins may relate to a unique life history profile (e.g., Hogg et al., 2020).

Mean RP scales positively and significantly with relative encephalization (endocranial volume / body mass) when just hominins are considered (Hogg et al., 2020). Relative encephalization for *H. naledi* is 13.2 calculated from an endocranial volume of 535.0 mL and body mass of 40.5 kg (mean values calculated from Garvin et al., 2017; Hawks et al., 2017; Holloway et al., 2018). When *H. naledi* is included in a regression analysis of log-transformed mean RP and mean encephalization of hominins, the relationship is not significant (linear  $r = 0.209$ ,  $p = 0.539$ ). This occurs because *H. naledi* does not scale as expected (Figure 7). When *H. naledi* is removed, the relationship is significant ( $r = 0.714$ ,  $p = 0.020$ ).

Other than Neandertal and *P. robustus*, most fossil hominin species are currently represented by a few RP values. As sample sizes increase future studies can determine if the relatively high RP we observed in *H. naledi* is characteristic of this species, and if this points towards a life history signal that differs compared to other hominins with lower RPs. Based on the few RP values we report, it would seem likely that the biological pathway that links mean RP to encephalization is different for *H. naledi* (Figure 7). An RP closer to seven days might have been expected, rather than nine or 11 days, given that *H. naledi* has an encephalization quotient that is similar to *Australopithecus* (Garvin et al., 2017). Yet, even though *H. naledi* has an australopith-sized brain, it shared aspects of brain organization with larger-brained species of *Homo* (*H. habilis*, *H. rudolfensis*, *H. erectus*, *H. sapiens*) (Holloway et al., 2018). It is possible that the shared aspects of neuroanatomy may indicate shared behaviors related to life history. Future studies might investigate if information from endocast morphology is important for understanding the disassociation we observed between RP and encephalization.

It is important to recognize that we have not considered the full spectrum of the capacity of mammalian ameloblasts (e.g., Ungar, 2015). The terms “relatively fast” or “slow” have been applied here to the enamel growth of fossil hominins. But hominin enamel growth can represent the slow end of a continuum among mammals. In wild boar for example, DSR values can centre around 20  $\mu\text{m}/\text{day}$  in the outer enamel of molars (Kierdorf et al., 2019). Molar

enamel extension rates of domestic pig can reach over 300  $\mu\text{m}/\text{day}$  (Emken et al., 2023). In this context, the “fast” enamel growth rates of some australopiths would be quite slow.

#### 4.4 | Dental development of *H. naledi*

Our histology study adds new information about the dental development of *H. naledi*. On average, enamel was secreted slightly faster in two canines and a molar compared to recent humans and *H. erectus*, but the fast DSRs present in some australopiths and *Paranthropus* were not present in *H. naledi*. The canine formed over a long and ‘human like’ period with a very slow rate of extension in cervical enamel. When considered alongside previous research, these findings indicate that the dental development of *H. naledi* has a mosaic ontogeny, with enamel growth that resembles recent humans combined with aspects of tooth emergence that are both modern and more primitive.

#### AUTHOR CONTRIBUTIONS

**Patrick Mahoney:** Conceptualization (equal); formal analysis (lead); investigation (equal); writing – original draft (lead). **Gina McFarlane:** Investigation (equal); writing – review and editing (equal). **Alberto J. Taurozzi:** Investigation (equal). **Palesa P. Madupe:** Investigation (equal). **Mackie C. O’Hara:** Investigation (equal); writing – review and editing (equal). **Keneiloe Molopyane:** Investigation (equal); writing – review and editing (equal). **Enrico Cappellini:** Conceptualization (equal); investigation (equal); writing – review and editing (equal). **John Hawks:** Conceptualization (equal); investigation (equal); writing – review and editing (equal). **Matthew M. Skinner:** Conceptualization (equal); investigation (equal); writing – review and editing (equal). **Lee Berger:** Conceptualization (equal); investigation (equal); writing – review and editing (equal).

#### ACKNOWLEDGMENTS

For access to the *H. naledi* remains we thank the South African Heritage Resource Agency and, for facilitating the movement of the material, Curator of Collections Bernard Zipfel (University of Witwatersrand).

#### FUNDING INFORMATION

Funding for the excavation and recovery of the material was from the National Geographic Society and the Lyda Hill Foundation. Support for transportation of the specimens was from the Lee R Berger Foundation for Exploration. PM acknowledges support from The Royal Society and The Leverhulme Trust (grant numbers RG110435 and RPG-2018-226). The participation of MMS was supported by the European Research Council (ERC) under the European Union’s Horizon 2020 research and innovation programme (grant agreement No. 819960). PPM and EC are supported by the European Commission through the Marie S. Curie European Training Network ‘PUSHH’ (grant number 861389). AJT, LB, JH and EC are supported by the European Research Council (ERC) under the European Union’s Horizon 2020 research and innovation program

(grant number 101021361). The participation of MCO was supported by the ERC under the Horizon 2020-MSCA-IF-2020 (grant agreement No. 101026776).

## CONFLICT OF INTEREST STATEMENT

The authors declare no conflict of interest.

## DATA AVAILABILITY STATEMENT

Raw data are available in the Tables (main text) and the Supplementary Tables.

## ORCID

Patrick Mahoney  <https://orcid.org/0000-0002-2715-3096>

Gina McFarlane  <https://orcid.org/0000-0002-7441-2281>

John Hawks  <https://orcid.org/0000-0003-3187-3755>

## REFERENCES

- Antoine, D., Hillson, S., & Dean, M. C. (2009). The developmental clock of dental enamel: A test for the periodicity of prism cross-striations in modern humans and an evaluation of the most likely sources of error in histological studies of this kind. *Journal of Anatomy*, 214(1), 45–55. <https://doi.org/10.1111/j.1469-7580.2008.01010.x>
- Aris, C., Mahoney, P., O'Hara, M. C., & Deter, C. (2020). Enamel thickness and growth rates in modern human permanent first molars over a 2000 year period in Britain. *American Journal of Physical Anthropology*, 173(1), 141–157. <https://doi.org/10.1002/ajpa.24026>
- Bailey, S. E., Brophy, J. K., Moggi-Cecchi, J., & Deleuzene, L. K. (2019). The deciduous dentition of *Homo naledi*: A comparative study. *Journal of Human Evolution*, 136, 102655. <https://doi.org/10.1016/j.jhevol.2019.102655>
- Berger, L. R., Hawks, J., de Ruiter, D. J., Churchill, S. E., Schmid, P., Deleuzene, L. K., Kivell, T. L., Garvin, H.M., Williams, S.A., DeSilva, J.M., Skinner, M. M., Musiba, C.M., Cameron, N., Holliday, T.W., Harcourt-Smith, W., Ackermann, R. R., Bastir, M., Bogin, B., ... Zipfel, B. (2015). *Homo naledi*, a new species of the genus *Homo* from the Dinaledi chamber. *South Africa. Elife*, 4, e09560. <https://doi.org/10.7554/eLife.09560>
- Berthaume, M. A., Deleuzene, L. K., & Kupczik, K. (2018). Dental topography and the diet of *Homo naledi*. *Journal of Human Evolution*, 118, 14–26. <https://doi.org/10.1016/j.jhevol.2018.02.006>
- Beynon, A. D., Dean, M. C., & Reid, D. J. (1991). On thick and thin enamel. *American Journal of Physical Anthropology*, 86, 295–309. <https://doi.org/10.1002/ajpa.1330860216>
- Bolter, D. R., & Cameron, N. (2020). Utilizing auxology to understand ontogeny of extinct hominins: A case study on *Homo naledi*. *American Journal of Physical Anthropology*, 173, 368–380. <https://doi.org/10.1002/ajpa.24088>
- Bolter, D. R., Elliott, M. C., Hawks, J., & Berger, L. R. (2020). Immature remains and the first partial skeleton of a juvenile *Homo naledi*, a late middle Pleistocene hominin from South Africa. *PLoS One*, 15, e0230440. <https://doi.org/10.1371/journal.pone.0230440>
- Boyde, A. (1989). Enamel. In A. Oksche & L. Vollrath (Eds.), *Handbook of microscopic anatomy* (Vol. V/6, pp. 309–473). Teeth. Springer-Verlag.
- Bromage, T. G., & Dean, M. C. (1985). Re-evaluation of the age at death of immature fossil hominids. *Nature*, 317(6037), 525–527. <https://doi.org/10.1038/317525a0>
- Bromage, T. G., Hogg, R. T., Lacruz, R. S., & Hou, C. (2012). Primate enamel evinces long period biological timing and regulation of life history. *Journal of Theoretical Biology*, 305, 131–144. <https://doi.org/10.1016/j.jtbi.2012.04.007>
- Bromage, T. G., Lacruz, R. S., Hogg, R., Goldman, H. M., McFarlin, S. C., Warsaw, J., Dirks, W., Perez-Ochoa, A., Smolyar, I., Enlow, D. H., & Boyde, A. (2009). Lamellar bone is an incremental tissue reconciling enamel rhythms, body size, and organismal life history. *Calcified Tissue International*, 84, 388–404. <https://doi.org/10.1007/s00223-009-9221-2>
- Cofran, Z., & Walker, C. S. (2017). Dental development in *Homo naledi*. *Biology Letters*, 13, 20170339. <https://doi.org/10.1098/rsbl.2017.0339>
- Davies, T. W., Deleuzene, L. K., Gunz, P., Hublin, J. J., Berger, L. R., Gidna, A., & Skinner, M. M. (2020). Distinct mandibular premolar crown morphology in *Homo naledi* and its implications for the evolution of homo species in southern Africa. *Science Reports*, 10, 13196. <https://doi.org/10.1038/s41598-020-69993-x>
- Dean, C., Leakey, M. G., Reid, D., Schrenk, F., Schwartz, G. T., Stringer, C., & Walker, A. (2001). Growth processes in teeth distinguish modern humans from *Homo erectus* and earlier hominins. *Nature*, 414(6864), 628–631. <https://doi.org/10.1038/414628>
- Dean, M. C. (1998). A comparative study of cross striation spacings in cuspal enamel and of four methods of estimating the time taken to grow molar cuspal enamel in *pan*, *pongo* and *homo*. *Journal of Human Evolution*, 35, 449–462. <https://doi.org/10.1006/jhevol.1998.0208>
- Dean, M. C. (2009). Extension rates and growth in tooth height of modern human and fossil hominin canines and molars. *Frontiers of Oral Biology*, 13, 68–73. <https://doi.org/10.1159/000242394>
- Dean, M. C., & Beynon, A. D. (1991). Histological reconstruction of crown formation time and initial root formation times in a modern human child. *American Journal of Physical Anthropology*, 86, 215–228.
- Dean, M. C., Beynon, A. D., Thackeray, J. F., & Macho, G. A. (1993). Histological reconstruction of dental development and age at death of a juvenile *Paranthropus robustus* specimen, SK 63, from Swartkrans, South Africa. *American Journal of Physical Anthropology*, 91, 401–419.
- Dean, M. C., & Vesey, P. (2008). Preliminary observations on increasing root length during the eruptive phase of tooth development in modern humans and great apes. *Journal of Human Evolution*, 54, 258–271.
- Deleuzene, L. K., Skinner, M. M., Bailey, S. E., Brophy, J. K., Elliott, M. C., Gurtov, A., Irish, J. D., Moggi-Cecchi, J., de Ruiter, D. J., Hawks, J., & Berger, L. R. (2023). Descriptive catalog of *Homo naledi* dental remains from the 2013 to 2015 excavations of the Dinaledi chamber, site U.W. 101, within the rising star cave system, South Africa. *Journal of Human Evolution*, 23, 180. <https://doi.org/10.1016/j.jhevol.2023.103372>
- Dirks, P. H., Roberts, E. M., Hilbert-Wolf, H., Kramers, J. D., Hawks, J., Dosseto, A., Duval, M., Elliott, M., Evans, M., Grün, R., Hellstrom, J., Herries, A. I., Joannes-Boyau, R., Makhubela, T. V., Placzek, C. J., Robbins, J., Spandler, C., Wiersma, J., Woodhead, J., ... Berger, L. R. (2017). The age of *Homo naledi* and associated sediments in the rising star cave. *South Africa. In Elife*, 6, e24231. <https://doi.org/10.7554/eLife.24231>
- Elliott, M. C., Makhubela, T. V., Brophy, K. J., Churchill, S. E., Peixotto, B., Feuerriegel, E. M., Morris, H., Hunter, R., Tucker, S., Van Rooyen, D., Ramalepa, M., Tsikoane, M., Kruger, A., Spandler, C., Kramers, J., Roberts, E., Dirks, P. H. G. M., Hawks, J., & Berger, L. (2021). Expanded Explorations of the Dinaledi Subsystem, Rising Star Cave System, South Africa. *PaleoAnthropology*, 1, 15–22.
- Emken, S., Witzel, C., Kierdorf, U., Frölich, K., & Kierdorf, H. (2023). Wild boar versus domestic pig—deciphering of crown growth in porcine second molars. *Journal of Anatomy*, 242(6), 1078–1095. <https://doi.org/10.1111/joa.13838>
- Feuerriegel, E. M., Green, D. J., Walker, C. S., Schmid, P., Hawks, J., Berger, L. R., & Churchill, S. E. (2017). The upper limb of *Homo naledi*. *Journal of Human Evolution*, 104, 155–173. <https://doi.org/10.1016/j.jhevol.2016.09.013>
- Garvin, H. M., Elliott, M. C., Deleuzene, L. K., Hawks, J., Churchill, S. E., Berger, L. R., & Holliday, T. W. (2017). Body size, brain size, and sexual dimorphism in *Homo naledi* from the Dinaledi chamber. *Journal of Human Evolution*, 111, 119–138. <https://doi.org/10.1016/j.jhevol.2017.06.010>

- Guatelli-Steinberg, D., Floyd, B. A., Dean, M. C., & Reid, D. J. (2012). Enamel extension rate patterns in modern human teeth: Two approaches designed to establish an integrated comparative context for fossil primates. *Journal of Human Evolution*, 63, 475–486. <https://doi.org/10.1016/j.jhevol.2012.05.006>
- Guatelli-Steinberg, D., O'Hara, M. C., Le Cabec, A., Delezene, L. K., Reid, D. J., Skinner, M. M., & Berger, L. R. (2018). Patterns of lateral enamel growth in *Homo naledi* as assessed through perikymata distribution and number. *Journal of Human Evolution*, 121, 40–54. <https://doi.org/10.1016/j.jhevol.2018.03.007>
- Guatelli-Steinberg, D., Reid, D. J., Bishop, T. A., & Larsen, C. S. (2005). Anterior tooth growth periods in neandertals were comparable to those of modern humans. *Proceedings of the National Academy of Science USA*, 102(14197–14), 202–202. <https://doi.org/10.1073/pnas.0503108102>
- Harcourt-Smith, W. E., Throckmorton, Z., Congdon, K. A., Zipfel, B., Deane, A. S., Drapeau, M. S., Churchill, S. E., Berger, L. R., & DeSilva, J. M. (2015). The foot of *Homo naledi*. *Nature Communications*, 6, 8432. <https://doi.org/10.1038/ncomms9432>
- Harvati, K., & Reyes-Centeno, H. (2022). Evolution of homo in the middle and late Pleistocene. *Journal of Human Evolution*, 173, 103279. <https://doi.org/10.1016/j.jhevol.2022.103279>
- Hawks, J., Elliott, M., Schmid, P., Churchill, S. E., Ruitter, D. J., Roberts, E. M., Hilbert-Wolf, H., Garvin, H. M., Williams, S. A., Delezene, L. K., Feuerriegel, E. M., Randolph-Quinney, P., Kivell, T. L., Laird, M. F., Tawane, G., DeSilva, J. M., Bailey, S. E., Brophy, J. K., Meyer, M. R., ... Berger, L. R. (2017). New fossil remains of *Homo naledi* from the Lesedi chamber, South Africa. *eLife*, 9, e24232. <https://doi.org/10.7554/eLife.24232>
- Hogg, R., Lacruz, R., Bromage, T. G., Dean, M. C., Ramirez-Rozzi, F., Girmurugan, S. B., McGrosky, A., & Schwartz, G. T. (2020). A comprehensive survey of Retzius periodicities in fossil hominins and great apes. *Journal of Human Evolution*, 149, 102896. <https://doi.org/10.1016/j.jhevol.2020.102896>
- Holloway, R. L., Hurst, S. D., Garvin, H. M., Schoenemann, P. T., Vanti, W. B., Berger, L. R., & Hawks, J. (2018). Endocast morphology of *Homo naledi* from the Dinaledi chamber, South Africa. *Proceedings of the National Academy of Science USA*, 115(22), 5738–5743. <https://doi.org/10.1073/pnas.1720842115>
- Hublin, J. J., Ben-Ncer, A., Bailey, S., Freidline, S. E., Neubauer, S., Skinner, M. M., Bergmann, I., Le Cabec, A., Benazzi, S., Harvati, K., & Gunz, P. (2017). New fossils from jebel Irhoud, Morocco and the pan-African origin of *Homo sapiens*. *Nature*, 546, 289–292. <https://doi.org/10.1038/nature22336>
- Irish, J. D., Bailey, S. E., Guatelli-Steinberg, D., Delezene, L. K., & Berger, L. R. (2018). Ancient teeth, phenetic affinities, and African hominins: Another look at where *Homo naledi* fits in. *Journal of Human Evolution*, 122, 108–123. <https://doi.org/10.1016/j.jhevol.2018.05.007>
- Kierdorf, H., Breuer, F., Witzel, C., & Kierdorf, U. (2019). Pig enamel revisited - incremental markings in enamel of wild boars and domestic pigs. *Journal of Structural Biology*, 205(1), 48–59.
- Kivell, T. L., Deane, A. S., Tocheri, M. W., Orr, C. M., Schmid, P., Hawks, J., Berger, L. R., & Churchill, S. E. (2015). The hand of *Homo naledi*. *Nature Communications*, 6, 8431. <https://doi.org/10.1038/ncomms9431>
- Kupczik, K., & Skinner, M. M. (2018). Mandibular molar root morphology in *Homo naledi*. Paper presented at the 87th annual American Association of Physical Anthropology Meeting, Austin, Texas. [https://pure.mpg.de/pubman/faces/ViewItemOverviewPage.jsp?itemId=item\\_2596640](https://pure.mpg.de/pubman/faces/ViewItemOverviewPage.jsp?itemId=item_2596640)
- Lacruz, R., & Bromage, T. (2006). Appositional enamel growth in molars of south African fossil hominids. *Journal of Anatomy*, 209, 13–20. <https://doi.org/10.1111/j.1469->
- Lacruz, R. S. (2007). Enamel microstructure of the hominid KB 5223 from Kromdraai, South Africa. *American Journal of Physical Anthropology*, 132, 175–178. <https://doi.org/10.1002/ajpa.20506>
- Lacruz, R. S., Dean, M. C., Ramirez-Rozzi, F., & Bromage, T. G. (2008). Megadontia, striae periodicity and patterns of enamel secretion in Plio-Pleistocene fossil hominins. *Journal of Anatomy*, 213, 148–158. <https://doi.org/10.1111/j.1469-7580.2008.00938.x>
- Laird, M. F., Schroeder, L., Garvin, H. M., Scott, J. E., Dembo, M., Radovčić, D., Musiba, C. M., Ackermann, R. R., Schmid, P., Hawks, J., Berger, L. R., & de Ruitter, D. J. (2017). The skull of *Homo naledi*. *Journal of Human Evolution*, 104, 100–123. <https://doi.org/10.1016/j.jhevol.2016.09.009>
- Li, C., & Risnes, S. (2004). SEM observations of Retzius lines and prism cross-striations in human dental enamel after different acid etching regimes. *Archives of Oral Biology*, 49, 45–52.
- Lockey, A. L., Alemseged, Z., Hublin, J. J., & Skinner, M. M. (2020). Maxillary molar enamel thickness of Plio-Pleistocene hominins. *Journal of Human Evolution*, 142, 102731. <https://doi.org/10.1016/j.jhevol.2019.102731>
- Mahoney, P. (2008). Intraspecific variation in M1 enamel development in modern humans: Implications for human evolution. *Journal of Human Evolution*, 55, 131–147. <https://doi.org/10.1016/j.jhevol.2008.02.004>
- Mahoney, P. (2015). Dental fast track: Prenatal enamel growth, incisor eruption, and weaning in human infants. *American Journal of Physical Anthropology*, 156, 407–421. <https://doi.org/10.1002/ajpa.22666>
- Mahoney, P., McFarlane, G., Loch, C., White, S., Floyd, B., Dunn, E. C., Pitfield, R., Nava, A., & Guatelli-Steinberg, D. (2022). Dental biorhythm is associated with adolescent weight gain. *Communications Medicine*, 2, 99. <https://doi.org/10.1038/s43856-022-00164->
- Mahoney, P., McFarlane, G., Pitfield, R., O'Hara, M. C., Miskiewicz, J. J., Seal, H., Deter, C., & Guatelli-Steinberg, D. (2020). A structural biorhythm related to human sexual dimorphism. *Journal of Structural Biology*, 211, 107550. <https://doi.org/10.1016/j.jsb.2020.107550>
- Mahoney, P., McFarlane, G., Smith, B. H., Miskiewicz, J. J., Cerrito, P., Liversidge, H., Mancini, L., Dreossi, D., Veneziano, A., Bernardini, F., Cristiani, E., Behie, A., Coppa, A., Bondioli, L., Frayer, D.W., Radovčić, D., & Nava, A. (2021). Growth of Neanderthal infants from Krapina (120–130 ka), Croatia. *Proceedings of the Royal Society B. Biological Sciences*, 288, 20212079. <https://doi.org/10.1098/rspb.2021.2079>
- Mahoney, P., Smith, T., Schwartz, G., Dean, C., & Kelley, J. (2007). Molar crown formation in the late Miocene Asian hominoids, *Sivapithecus parvada* and *Sivapithecus sivalensis*. *Journal of Human Evolution*, 53, 61–66. <https://doi.org/10.1016/j.jhevol.2007.01.007>
- Marchi, D., Walker, C. S., Wei, P., Holliday, T. W., Churchill, S. E., Berger, L. R., & DeSilva, J. M. (2017). The thigh and leg of *Homo naledi*. *Journal of Human Evolution*, 104, 174–204. <https://doi.org/10.1016/j.jhevol.2016.09.005>
- McFarlane, G., Guatelli-Steinberg, D., Loch, C., White, S., Bayle, P., Floyd, B., Pitfield, R., & Mahoney, P. (2021). An inconstant biorhythm: The changing pace of Retzius periodicity in human permanent teeth. *American Journal of Physical Anthropology*, 175, 172–186. <https://doi.org/10.1002/ajpa.24206>
- McFarlane, G., Littleton, J., & Floyd, B. (2014). Estimating striae of Retzius periodicity nondestructively using partial counts of perikymata: Estimating periodicity non-destructively. *American Journal of Biological Anthropology*, 154, 251–258.
- Modesto-Mata, M., Dean, M. C., Lacruz, R. S., Bromage, T. G., Garcia-Campos, C., Martinez de Pinillos, M., Martín-Francis, L., Martín-Torres, M., Carbonell, E., Arsuaga, J. L., & Bermudez de Castro, J. M. (2020). Short and long period growth markers of enamel formation distinguish European Pleistocene hominins. *Scientific Reports*, 10, 4665. <https://doi.org/10.1038/s41598-020-61659-y>
- O'Hara, M. C. (2021). Features of catarrhine posterior dental crowns associated with durophagy: Implications for fossil hominins. (PhD), Ohio State University.
- O'Hara, M. C., & Guatelli-Steinberg, D. (2022). Reconstructing tooth crown heights and enamel caps: A comparative test of three existing methods with recommendations for their use. *Anatomical Record (Hoboken)*, 305, 123–143.

- O'Hara, M. C., Skinner, M. M., & Guatelli-Steinberg, D. (2019). Comparative two-dimensional relative enamel thickness (RET) of south African hominin premolars. Paper presented at the 88th Annual Meeting of the American Association of Physical Anthropologists: American Journal of Physical Anthropology. <https://onlinelibrary.wiley.com/toc/10968644/2019/168/S68>
- Ramirez Rozzi, F. V., & Bermudez de Castro, J. M. (2004). Surprisingly rapid growth in Neanderthals. *Nature*, 428, 936–939. <https://doi.org/10.1038/nature02428>
- Reid, D. J., Beynon, A. D., & Ramirez Rozzi, F. V. (1998). Histological reconstruction of dental development in four individuals from a medieval site in Picardie, France. *Journal of Human Evolution*, 35, 463–477. <https://doi.org/10.1006/jhev.1998.0233>
- Reid, D. J., & Dean, M. C. (2006). Variation in modern human enamel formation times. *Journal of Human Evolution*, 50, 329–346. <https://doi.org/10.1016/j.jhevol.2005.09.003>
- Reid, D. J., & Ferrell, R. J. (2006). The relationship between number of striae of Retzius and their periodicity in imbricational enamel formation. *Journal of Human Evolution*, 50, 195–202. <https://doi.org/10.1016/j.jhevol.2005.09.002>
- Retzius, A. (1837). Bemerkungenq ber den inneren Bau der Zahne, mit besonderer Rucksicht auf dem in Zahnknochen Vorkommenden Reohrenbau. *Archives of Anatomy and Physiology*, 1837, 486–566.
- Risnes, S. (1986). Enamel apposition rate and the prism periodicity in human teeth. *Scandinavian Journal of Dental Research*, 94(5), 394–404. <https://doi.org/10.1111/j.1600-0722.1986.tb01779.x>
- Robbins, J. L., Dirks, P. H. G. M., Roberts, E. M., Kramers, J. D., Makhubela, T. V., Hilbert-Wolf, H. L., Elliott, M., Wiersma, J. P., Placzek, C. J., Evans, M., & Berger, L. R. (2021). Providing context to the *Homo naledi* fossils: Constraints from flowstones on the age of sediment deposits in rising star cave, South Africa. *Chemical Geology*, 567, 120108. <https://doi.org/10.1016/j.chemgeo.2021.120108>
- Rosas, A., Ros, L., Estalrich, A., Liversidge, H., Garca-Taberner, A., Huguet, R., Cardoso, H., Bastir, M., Lalueza-Fox, C., de la Rasilla, M., & Dean, C. (2017). The growth pattern of neandertals, reconstructed from a juvenile skeleton from El Sidrn (Spain). *Science*, 357, 1282–1287. <https://doi.org/10.1126/science.aan6463>
- Schour, I., & Poncher, H. G. (1937). Rate of apposition of enamel and dentin, measured by the effect of acute fluorosis. *American Journal of Diseases of Children*, 54, 757–776.
- Schroeder, L., Scott, J. E., Garvin, H. M., Laird, M. F., Dembo, M., Radovi, D., Berger, L. R., de Ruiter, D. J., & Ackermann, R. R. (2017). Skull diversity in the homo lineage and the relative position of *Homo naledi*. *Journal of Human Evolution*, 104, 124–135. <https://doi.org/10.1016/j.jhevol.2016.09.014>
- Schwartz, G. T., Liu, W., & Zheng, L. (2003). Preliminary investigation of dental microstructure in the Yuanmou hominoid (*Lufengpithecus hudienensis*), Yunnan Province, China. *Journal of Human Evolution*, 44, 189–202.
- Schwartz, G. T., Reid, D. J., & Dean, C. (2001). Developmental aspects of sexual dimorphism in hominoid canines. *International Journal of Primatology*, 22, 837–860. <https://doi.org/10.1023/A:1012073601808>
- Shellis, R. P. (1984). Variations in growth of the enamel crown in human teeth and a possible relationship between growth and enamel structure. *Archives of Oral Biology*, 29, 697–705.
- Skinner, M. M., Alemseged, Z., Gaunitz, C., & Hublin, J. J. (2015). Enamel thickness trends in Plio-Pleistocene hominin mandibular molars. *Journal of Human Evolution*, 85, 35–45. <https://doi.org/10.1016/j.jhevol.2015.03.012>
- Skinner, M. M., Lockley, A., Gunz, P., Hawks, J., & Deleuzene, L. K. (2016). Enamel-dentine junction morphology and enamel thickness of the Dinaledi dental collection. In Paper presented at the 85th annual meeting of the American Association of Physical Anthropology. American Journal of Biological Anthropology.
- Smith, B. H. (1989). Dental development as a measure of life history in primates. *Evolution*, 43, 683–688. <https://doi.org/10.1111/j.1558-5646.1989.tb04266.x>
- Smith, T. M. (2008). Incremental dental development: Methods and applications in hominoid evolutionary studies. *Journal of Human Evolution*, 54, 205–224. <https://doi.org/10.1016/j.jhevol.2007.09.020>
- Smith, T. M., Tafforeau, P., Le Cabec, A., Bonnin, A., Houssaye, A., Pouech, J., Moggi-Cecchi, J., Manthi, F., Ward, C., Makaremi, M., & Menter, C. G. (2015). Dental ontogeny in pliocene and early pleistocene hominins. *PLoS One*, 10(2), e0118118.
- Smith, T. M., Tafforeau, P., Reid, D. J., Grn, R., Eggins, S., Boutakiout, M., & Hublin, J. J. (2007). Earliest evidence of modern human life history in north African early *Homo sapiens*. *Proceeding of the National Academy of Science USA*, 104, 6128–6133. <https://doi.org/10.1073/pnas.0700747104>
- Smith, T. M., Tafforeau, P., Reid, D. J., Pouech, J., Lazzari, V., Zermeno, J. P., Guatelli-Steinberg, D., Olejniczak, A. J., Hoffman, A., Radovic, J., Makaremi, M., Toussaint, M., Stringer, C., & Hublin, J. J. (2010). Dental evidence for ontogenetic differences between modern humans and Neanderthals. *Proceedings of the National Academy of Science USA*, 107, 20923–20928. <https://doi.org/10.1073/pnas.1010906107>
- Towle, I., Irish, J. D., & De Groot, I. (2017). Behavioral inferences from the high levels of dental chipping in *Homo naledi*. *American Journal of Physical Anthropology*, 164, 184–192. <https://doi.org/10.1002/ajpa.23250>
- Ungar, P. S. (2015). Origins and functions of teeth: From “toothed” Worms to mammals. In D. Joel & G. Irish (Eds.), *Richard Scott* (pp. p19–p36). A Companion to Dental Anthropology.
- Ungar, P. S., & Berger, L. R. (2018). Brief communication: Dental micro-wear and diet of *Homo naledi*. *American Journal of Physical Anthropology*, 166, 228–235. <https://doi.org/10.1002/ajpa.23418>
- VanSickle, C., Cofran, Z., Garca-Martnez, D., Williams, S. A., Churchill, S. E., Berger, L. R., & Hawks, J. (2018). *Homo naledi* pelvic remains from the Dinaledi chamber, South Africa. *Journal of Human Evolution*, 125, 122–136. <https://doi.org/10.1016/j.jhevol.2017.10.001>
- Williams, S. A., Garca-Martnez, D., Bastir, M., Meyer, M. R., Nalla, S., Hawks, J., Schmid, P., Churchill, S. E., & Berger, L. R. (2017). The vertebrae and ribs of *Homo naledi*. *Journal of Human Evolution*, 104, 136–154. <https://doi.org/10.1016/j.jhevol.2016.11.003>
- Xing, S., Tafforeau, P., O'Hara, M., Modesto-Mata, M., Martn-Francs, L., Martn-Torres, M., Zhang, L., Schepartz, L.A., de Castro, J. M. B., & Guatelli-Steinberg, D. (2019). First systematic assessment of dental growth and development in an archaic hominin (genus, *homo*) from East Asia. *Science Advances*, 5(1), eaau0930. <https://doi.org/10.1126/sciadv.aau0930>
- Zheng, L., Seon, Y. J., Mouro, M. A., Schnell, S., Kim, D., Harada, H., Papagerakis, S., & Papagerakis, P. (2013). Circadian rhythms regulate amelogenesis. *Bone*, 55(1), 158–165. <https://doi.org/10.1016/j.bone.2013.02.011>

## SUPPORTING INFORMATION

Additional supporting information can be found online in the Supporting Information section at the end of this article.

**How to cite this article:** Mahoney, P., McFarlane, G., Taurozzi, A. J., Madupe, P. P., O'Hara, M. C., Molopyane, K., Cappellini, E., Hawks, J., Skinner, M. M., & Berger, L. (2024). Human-like enamel growth in *Homo naledi*. *American Journal of Biological Anthropology*, 1–14. <https://doi.org/10.1002/ajpa.24893>